# Electrical resistivity structure of the Flathead Basin in southeastern British Columbia, Canada[1]

JAGDISH C. GUPTA AND ALAN G. JONES
*Geological Survey of Canada, 1 Observatory Crescent, Ottawa, Ont., Canada K1A 0Y3*

Received October 18, 1989
Revision accepted April 6, 1990

In June 1985, wide-band magnetotelluric data were acquired at 12 equally spaced sites along a 30 km profile crossing the Flathead (Kishenehn) Basin in southeastern British Columbia, Canada. These data have been modelled by both one-dimensional inverse techniques and two-dimensional forward trial-and-error fitting. The results indicate the presence in the area of the following three major zones of low electrical resistivity (10–500 $\Omega \cdot$ m):
1. Sediments of the 10 km wide Flathead sedimentary basin, extending to a depth of about 2 km, dominate the responses in the middle of the profile.
2. In the eastern part of the profile, in the area of the Lewis Range, a thin ($\simeq$ 1 km) zone of low resistivity (35 $\Omega \cdot$ m) is imaged at a depth of some 3 km extending eastward from the edge of the basin. We associate this zone with the less dense thrusted Mesozoic clastic rocks lying directly below the Proterozoic rocks of the Lewis thrust sheet.
3. Beneath the Flathead Basin is a third zone, of higher resistivity (500 $\Omega \cdot$ m), which extends to deep within the crust. This zone may originate from mantle upflow, as recently proposed to explain the existence of Cordilleran conductors in other localities.
Additionally, to model the long-period geomagnetic transfer function responses, we are required to postulate the existence of a zone of low resistivity in the middle to lower crust, 50 km west of the survey line, corresponding to the location of the Rocky Mountain Trench.

---

En juin 1985, une large bande magnétotellurique a permis d'acquérir des données sur 12 sites, également espacés, le long d'une coupe de 30 km traversant le bassin de Flathead (Kishenehn), dans le sud-est de la Colombie-Britannique, Canada. Ces données ont servi à élaborer une modèle, à une dimension en utilisant les techniques d'inversion, et aussi à deux dimensions à partir d'approximations successives. Les résultats indiquent la présence dans la région des trois zones majeures de faible résistivité électriques (10–500 $\Omega \cdot$ m) qui suivent:
1. Les sédiments du bassin sédimentaire de Flathead de 10 km de largeur, d'une profondeur d'environ 2 km, lesquels sont responsables en majoritairement de la partie centrale de la coupe.
2. Dans la partie orientale de la coupe, région de Lewis Range, une zone peu épaisse ($\simeq$ 1 km) de faible résistivité (35 $\Omega \cdot$ m) est imagée à une profondeur de quelques 3 km, qui s'étend vers l'est en partant de la bordure du bassin. Cette zone est associée aux roches clastiques du Mésozoïque peu chevauchantes qui reposant directement sous les roches protérozoïques de la nappe de chevauchement de Lewis.
3. Une troisième zone est sous-jacente au bassin de Flathead, de résistivité plus forte (500 $\Omega \cdot$ m), et qui se prolonge profondément dans la croûte. Dans le but d'expliquer l'existence de conducteurs cordillériens dans d'autres loclités, il a été proposé récemment que cette zone est probablement due à des courants ascendants dans le manteau.
D'autre part, dans le but de modéliser les réponses de la fonction du transfert géomagnétique de longues périodes, il faut présumer l'existence d'une zone de faible résistivité, à 50 km à l'ouest de la ligne du levé, s'étendant du centre à la partie inférieure de la croûte, et correspondant à la localisation du Sillon des Rocheuses.

[Traduit par la revue]

Can. J. Earth Sci. **27**, 1061–1073 (1990)

## Introduction

The petroleum, natural gas, and coal industries have, of late, shown considerable interest in the crustal structure of southeastern British Columbia. This is reflected in increased geological mapping, increased seismic and drilling activity, and increased exploration for coal deposits in the area, and in the discovery of the Waterton gas field. In particular, in the vicinity of the Flathead sedimentary basin, the oil and gas potential of Mesozoic clastic sediments beneath the Proterozoic Lewis thrust sheet, which lies to the east of the basin, prompted exploration by Shell (Canada) Ltd. One major ambiguity in the interpretations of the seismic reflection data was whether these Mesozoic clastic rocks were present beneath the MacDonald Range to the west of the basin. The electrical resistivity structure of the area, which would supplement the gravity and seismic results and aid our understanding of the crustal structure of the region, was virtually unknown.

To address this deficiency, Shell contracted a survey for high-quality wide-band magnetotelluric (MT) data long a 30 km profile crossing the Flathead Basin between 144°15′W and 114°40′W longitudes just north of the International Boundary. This east–west profile is in the Eastern System of the Canadian Cordillera and consists of 12 stations, approximately equally spaced, two to the west of the basin, five to the east, and the rest within the basin; their locations are shown in Figs. 1 and 2.

In this paper we present the data from these 12 stations and illustrate that these data are highly complex at the longer periods exhibiting strong three-dimensional (3D) effects. An appropriate subset of the data is used to determine one-dimensional (1D) and two-dimensional (2D) resistivity models of predominantly the basin structure. Consideration is given not only to the MT parameters but also to the observed geomagnetic transfer functions.

## Geology

The survey area lies in the Rocky Mountain region of southeastern British Columbia near the border with Alberta. The region displays a strong northwest–southeast structural trend. On the basis of the very detailed discussion of the rock types by Price (1962), the survey area can be divided into three distinct zones (Fig. 1):

[1]Geological Survey of Canada Contribution 32189; Lithoprobe publication 157.

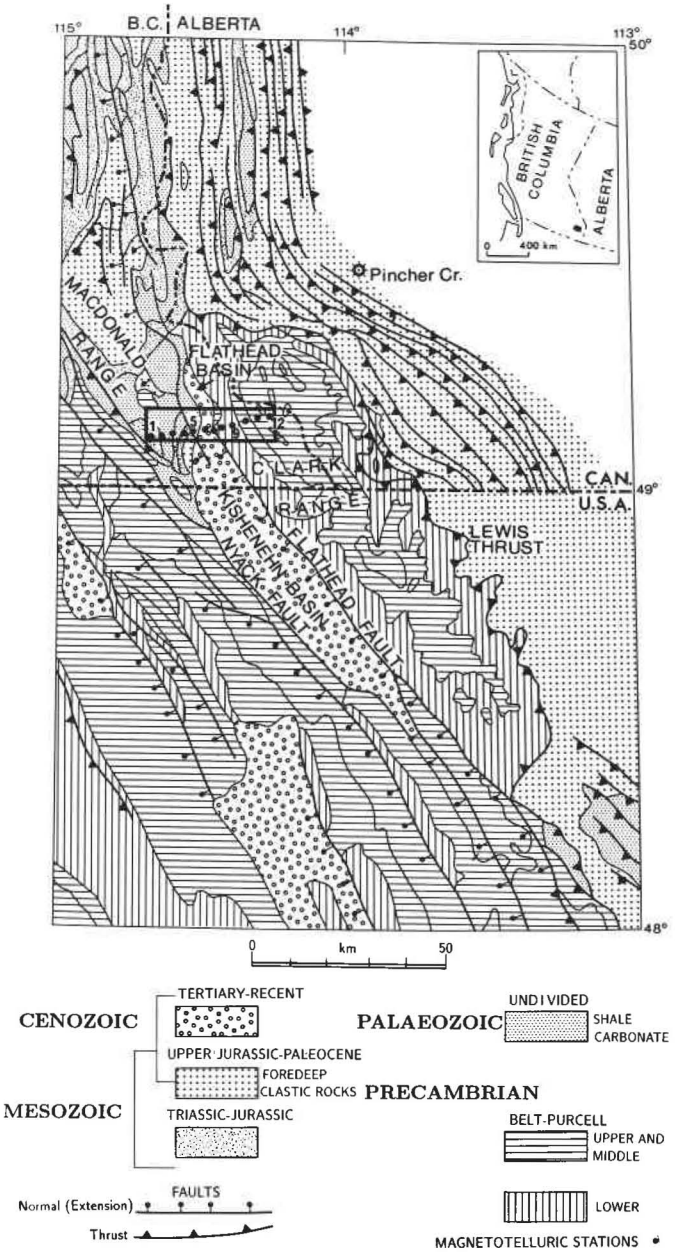


FIG. 1. Generalized geology map of southeastern British Columbia (from Price 1981) showing the survey area and approximate locations of the stations. The western part of the survey area lies in the MacDonald Range, the central part in the Flathead Basin, and the eastern part in the Clark Range of the Lewis thrust sheet.

1. *Western zone*: The western part of this zone lies in the region of the MacDonald Range and contains Paleozoic rocks. The eastern part is dominated by Triassic, Jurassic, and Cretaceous strata. The main rock types are mudstone, shale, siltstone, sandstone, conglomerate, coal, limestone, dolomite, dolomitic siltstones, volcanic breccia, and tuff.

2. *Central zone*: The central zone consists of the half-graben sedimentary Flathead Basin, which is bounded to the east by the Flathead Fault (a listric normal fault formed after the emplacement of the Lewis thrust sheet). The related Harvey Fault (Fig. 2) merges with the Flathead Fault southeast of our survey area.

The Flathead Basin forms the northern part of the Kishenehn Basin, which extends for over 100 km to the southeast from the Canada – United States border. The Kishenehn Basin is a half-graben bounded to the east and northeast by the Flathead Fault dipping 40° southwest, and to the southwest by the Nyack Fault dipping 45° northeast. The Flathead and Nyack faults are considered to be antithetic normal faults. Subsidence along these faults created an asymmetrical structural depression that contains approximately 3.4 km of nonmarine sediments of the Eocene–Oligocene (33 ± 1.5 Ma) Kishenehn Formation as well as Quaternary glacial and alluvial sediments. The sediments are thickest near the centre of the basin, and thin symmetrically to about 1 km adjacent to the bounding of faults. The maximum thickness of the sediments in the northern part of the basin is about 2.13 km (Bally *et al.* 1966).

Analysis of imbricated clasts in Kishenehn alluvial sediments indicates that the detritus originated in the footwall terrain of the Flathead Fault system (the Lewis thrust sheet, discussed below) and was transported to the southwest and deposited in the structural depression produced by the hanging-wall block. Alluvial fan, braided stream, flood basin, paludal, and lacustrine deposits typify Kishenehn sediments (Constenius 1988). The basin fill includes conglomerates, sandstones, siltstones, mudstones–claystones, marlstones, coals, and oil shales.

3. *Eastern zone*: This zone lies in the Clark Range and includes the Lewis thrust sheet, which is bounded by the Flathead Fault to the west and the much older Lewis thrust fault to the east. The maximum thickness of the thrust sheet preserved after Tertiary erosion is approximately 5 km. The major constituents of the thrust sheet are alluvial fan and megabreccia-landslide deposits (Constenius 1988). The Lewis thrust sheet has been reported to be older than the underlying structure in the footwall plate (Bally *et al.* 1966). In this regard, Constenius (1982) states that the Lewis thrust fault, which extends for about 457 km (Mudge and Earhart 1980) and formed in very late Paleocene to very early Eocene, placed a coherent slab of Proterozoic and lower Paleozoic rocks, 6–7 km thick (Childers 1964), onto a complexly deformed footwall of Paleozoic and Mesozoic strata. The Mesozoic strata are mainly Early Cretaceous in age and include rocks of the Crowsnest Formation and Blairemore Group, which are composed of volcanic breccia, sandstone, mudstone, siltstone, and pebble and cobble conglomerates.

The simplified geology of these three regions is shown in Fig. 2 together with a vertical cross section along line AB (from Price 1962). This section shows inferred approximate depths to rocks of various ages.

Examination of Bouguer gravity maps reveals pronounced gravity highs that are superimposed on the Lewis thrust sheet in the northeast and the MacDonald Range in the southwest, and a marked gravity low over the Kishenehn Basin lying between these two regions. This indicates abrupt density changes associated with Flathead and Nyack fault systems.

## Magnetotelluric data and analysis

The available data provided to us by Shell consisted of estimates of the four elements of the MT impedance tensor, **Z** from the 12 sites shown in Figs. 1 and 2, where

$$\mathbf{Z} = \begin{bmatrix} Z_{xx} & Z_{xy} \\ Z_{yx} & Z_{yy} \end{bmatrix}$$

and is a function of position, frequency, and rotation angle. The frequency range of acquisition was $9.5 \times 10^{-4}$ to 210 Hz, with reliable data in the range 0.01–100 Hz. At two sites (sites 4 and 6), estimates of error of the impedances were also provided.

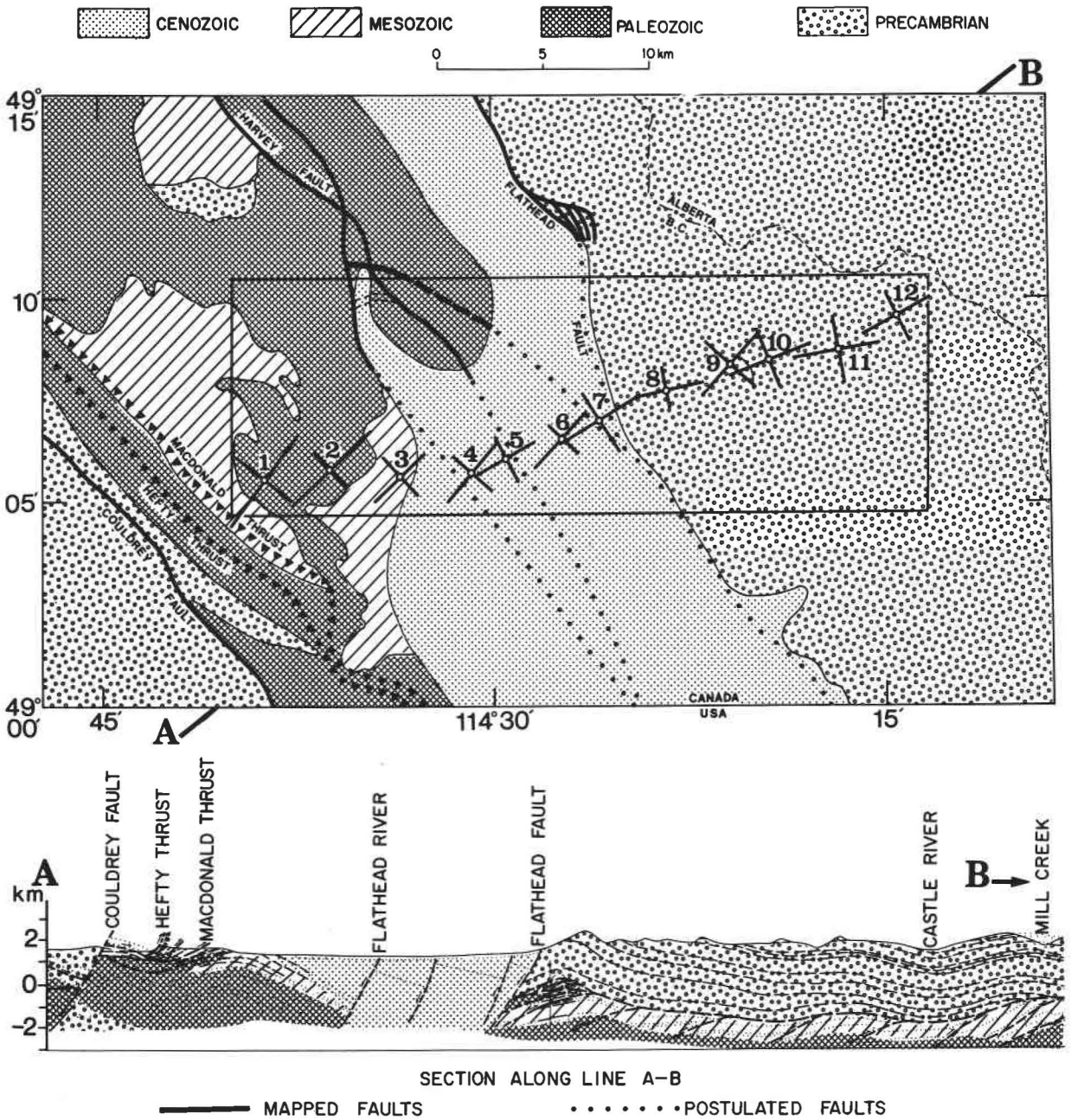


FIG. 2. Calculated average strike direction in the interval 0.1–10 Hz when the calculated skew values were noted to be low. The lengths of the bars in perpendicular directions are proportional to the average apparent resistivities. The strike directions align well with the northwest–southeast structural trend in the survey area.

These estimates were grouped into six frequency intervals to give a conservative estimate of the error within each interval, and then these six error estimates were assumed for all 12 stations. The error estimates ranged from 15% at the longest periods to 0.1% in the 3–100 Hz band.

The geomagnetic transfer function estimates, relating the vertical magnetic field to the two horizontal magnetic fields, and their errors (for all stations but one) were also provided.

The survey area is geologically complex, and 3D effects are evident in the data at the longer periods. This is shown in Fig. 3 for stations 1 and 2, where clearly the $\Phi_{yx}$ phases (in the measurement direction) go outside the $-180°$ to $-90°$ quadrant at periods longer than 10 s. Jones *et al.* (1988) also noted similar 3D effects at several MT stations in a region northwest of the present study area. In both cases, it is believed that large-scale east–west-flowing currents are strongly affected by gross resistive features—the Nelson batholith in the case of Jones *et al.* (1988) and the McDonald Range in this case.

The MT data were rotated into a uniform coordinate frame for all frequencies and for all sites. The direction of this coordinate system was chosen with reference to the dominant structural trend of the region, and with reference to the strike direction of the MT data in the frequency range 0.1–10 Hz. The strike direction chosen was N30°W geographic. In this coordinate system, the $x$-axis is N30°W and the $y$-axis is N60°E, which define the $\rho_{xy}$ and $\Phi_{xy}$ resistivity and phase estimates as representative of the E-polarization mode (TE) of induction, i.e., current flowing northwest–southeast, and the $\rho_{yx}$ and $\Phi_{yx}$

estimates as the B-polarization mode (TM), i.e., current flowing northeast–southwest. The responses from all 12 sites are illustrated in Fig. 4 (note that the $\Phi_{yx}$ phases have been rotated from the third quadrant to the first quadrant for comparison with the $\Phi_{yx}$ phases).

The skew values were found to be quite large at stations 1 and 2. At all other stations, skew values were low (often less than 02) in the interval 0.1–10 Hz, indicating that these stations may be less influenced by 3D structure. The strike directions derived from the data all lie within ~10° of the average values for low skew. These average values of the strike direction, and the direction perpendicular to it, are plotted in Fig. 2 and are seen to follow predominantly the geological trends in the area (the lengths of the bars are proportional to the logarithm of the average apparent resistivity in that direction). These strike directions justify rotating the resistivity and phase data into the dominant geological trends for the region (~N30°W). In the Plains of Alberta, Reddy and Rankin (1972) also found the major axis of resistivity anisotropy to be in a direction N30°W.

The survey data are affected by static shifts (Jones 1988; Sternberg *et al.* 1988). Such shifts become apparent when the $\Phi_{xy}$ and $\Phi_{yx}$ phase curves are similar and the apparent resistivity curves have the same shape but are at different levels. At high frequencies,the sedimentary basin stations 4, 5, and 7 do not show significant separation in their $\rho_{xy}$ and $\rho_{yx}$ estimates, and thus we conclude that they are relatively free of static shift effects. Other stations were found to have static-shifted data, especially stations 9–12. This observation, that MT data collected in sedimentary basins are less likely to be affected by static shift than data collected on very resistive terranes, is easily explained when one considers the greater attenuation of distortions (caused by near-surface inhomogeneities) by the less resistive sediments.

Recently, various authors have shown that apparent resistivity and phase curves calculated from two "invariant" impedances may provide responses that can be interpreted one dimensionally to give a reasonable approximation to the actual resistivity structure beneath a site even in the vicinity of quite strong 2D or 3D near-surface anomalies (Ingham 1988; Park and Livelybrooks 1989). These two impedances, (*i*) the Berdichevsky average $Z_{av}$ (Berdichevsky and Dmitriev 1976) and (*ii*) the determinant average $Z_{det}$ (Berdichevsky and Dmitriev 1976), are defined by

$$Z_{av} = (Z_{xy} - Z_{yx})/2; \qquad Z_{det} = (Z_{xx}Z_{yy} - Z_{xy}Z_{yx})^{1/2}$$

In a 2D Earth, $Z_{det}$ and $Z_{av}$ are the geometric and arithmetic means of the E- and B-polarization-mode responses, and also are the geometric and arithmetic means of the Eggers (1982) eigenstates $\lambda^+$ and $\lambda^-$. The determinant phase, $\Phi_{det}$, has the particular appeal that it is unaffected by galvanic charges on local near-surface inhomogeneities and can thus be considered free of static shift effects. Figure 5 illustrates the apparent resistivities and phases of the Berdichevsky and determinant averages. The determinant curves show a more consistent resemblance at nearby stations, and the phase curves are better confined. Thus, in our 1D modelling these data sets have been used. $Z_{det}$ has also been used by Sule and Hutton (1986) in the analysis of data from southeastern Scotland, and Hutton *et al* (1985) have shown that invariant responses can give interface depths closer to the results of 2D modelling than those obtained from E- and B-polarization responses. However, both Ingham (1988) and Ranganayaki (1984) noted that interpretation of deeper structures beneath sedimentary basins based on these invariant responses must be treated with caution, and they suggested modelling phase variations that are less influenced by static shifts.

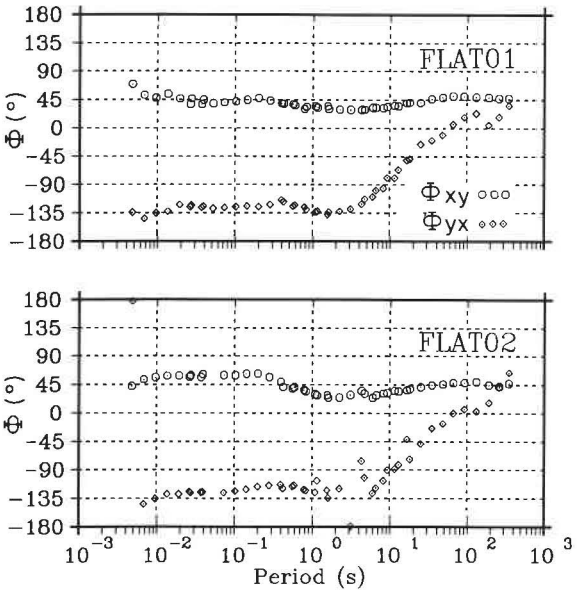


FIG. 3. The $\Phi_{xy}$ (circles) and $\Phi_{yx}$ (diamonds) phase responses from stations 1 and 2 located in the MacDonald Range. The $\Phi_{yx}$ phase is clearly affected by 3D structures for periods greater than 10 s, as the phase increases with increasing period to lie outside the −180° to −90° quadrant. The data at FLAT01 were acquired at an azimuth of 73° and at FLAT02 at an azimuth of 75°.

Geomagnetic transfer function analysis has been discussed and applied by various authors, for example, Schmucker (1970), Bailey *et al.* (1974), Jones (1981), and Gupta *et al.* (1983, 1985). The transfer functions can be plotted as arrows that identify induction anomalies by estimating the variations of the vertical component of the magnetic field caused by a laterally inhomogeneous Earth. One effective way of identifying conductive structures is to study the pseudosection of the transfer functions (e.g., Gough and Ingham 1983; Jones *et al* 1988). Such a pseudosection for the real transfer functions is shown in Fig. 6 for current flowing northwest–southeast, i.e., in the strike direction of the geology. The responses have been reversed to point in the direction of conductive structure (Jones 1986), and thus, on this figure, blue indicates conductive anomalies to the west, and red indicates anomalies to the east. At periods shorter than 3 s, the responses point strongly towards the Flathead Basin, located between stations 3 and 7. The red area at high frequencies below stations 10–12 suggests that the geomagnetic fields are being influenced by the shallow deposits of the less resistive sandstones and siltstones found in the nearby Phillips and Gateway formations (Price 1962) to the east, rather than the bulk of the material in the Lewis thrust sheet over which stations 9–12 are located. At ~10 s period, the red area beneath stations 9–12 probably reflects the influence of the Mesozoic strata (discussed below), extending far to the east. At the longest periods the responses from all stations strongly point westward, indicating the presence of a large anomaly of reduced resistivity in that direction. These results are substantiated by the quadrature transfer function pseudosection (not shown).

## One-dimensional models

It has been noted earlier that the $\rho_{det}$ and $\Phi_{det}$ curves from any station can be qualitative indicators of the electrical struc-

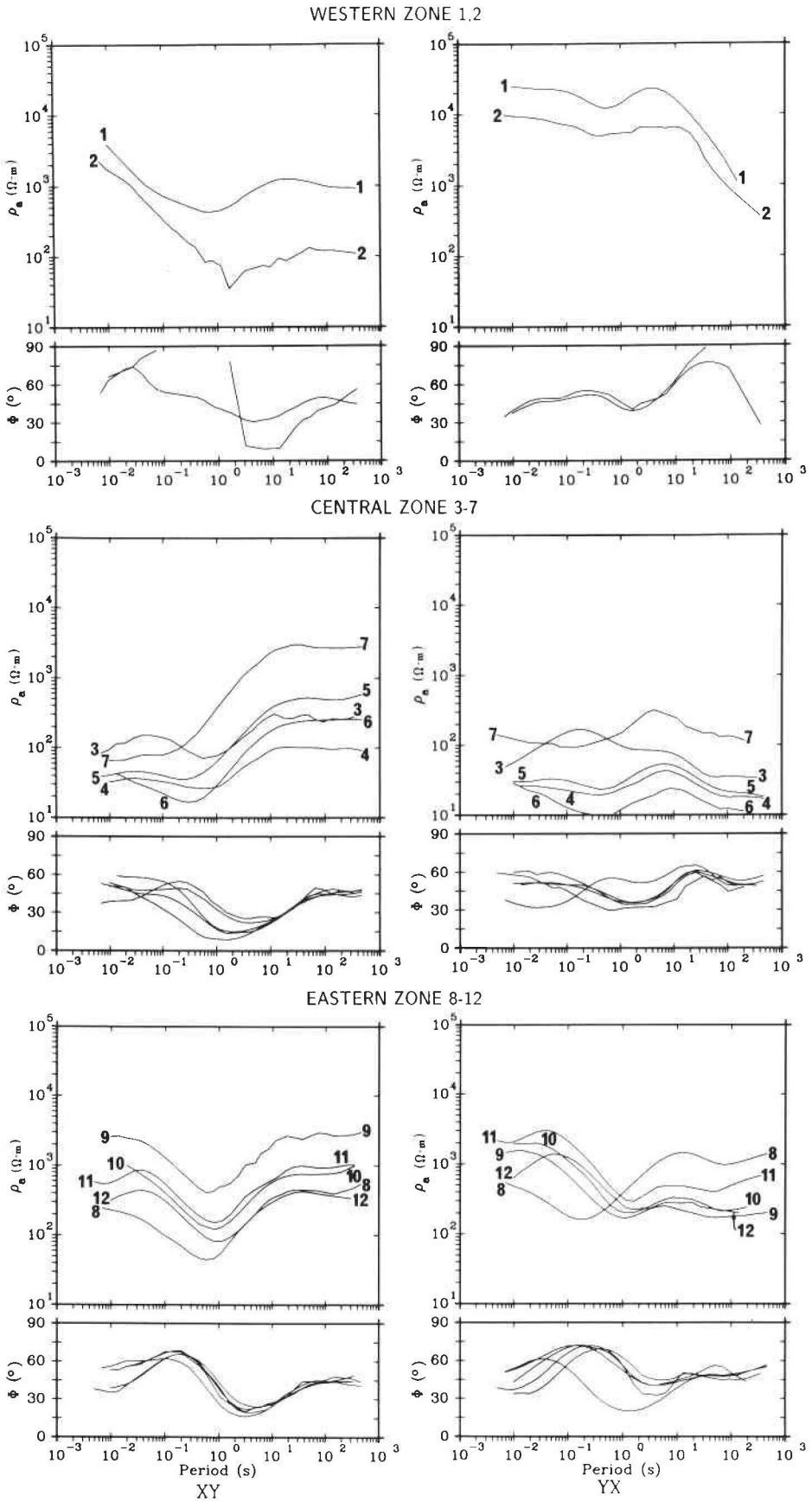


FIG. 4. Apparent resistivities and phases (reflected into the first quadrant) calculated in the azimuth of regional geological trends (nearly at 30°W of geographic north) in the survey area. Here $\rho_{xy}$ is in the direction of 30°W and $\rho_{yx}$ is in the direction of 60°E from geographic north.

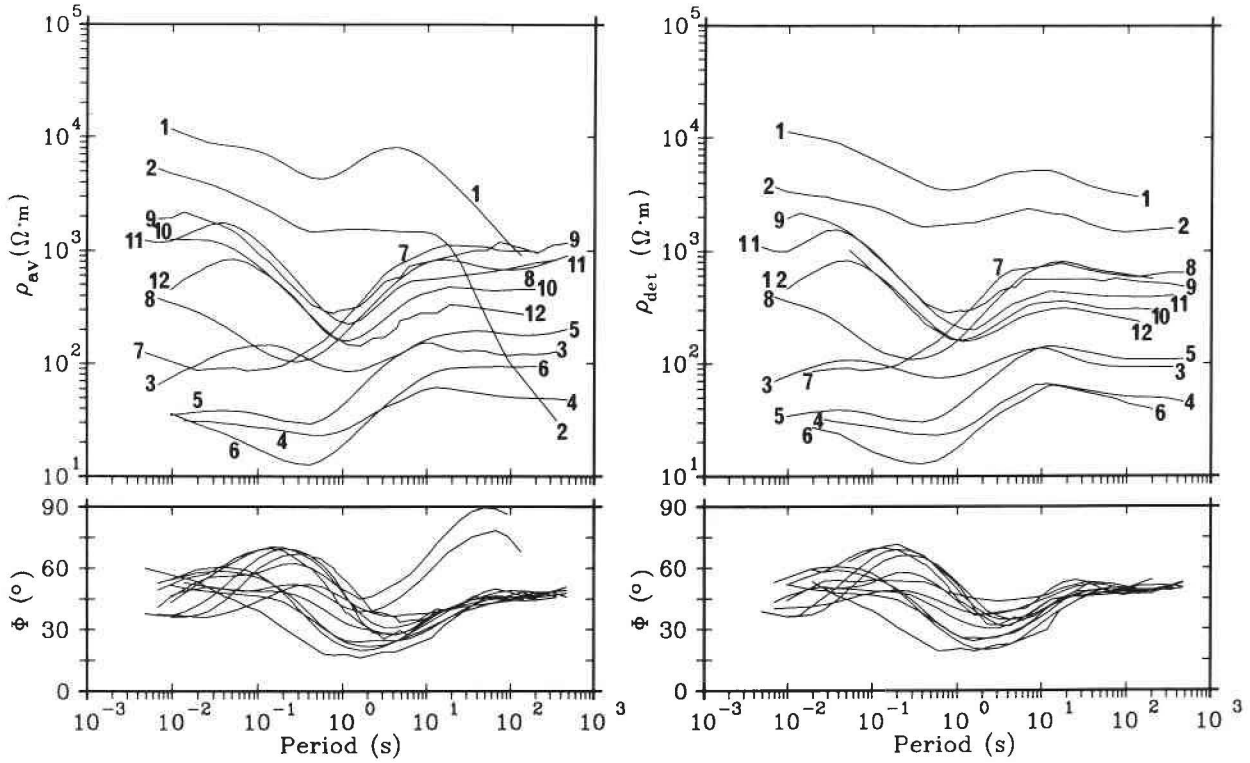


FIG. 5. Appparent resistivities and phases calculated from the Berdichevsky averages ($Z_{av}$) (left-hand side) and from the determinant averages ($Z_{det}$) (right-hand side) of the impedance tensor elements.

ture beneath it. One-dimensional inversions of the $\rho_{det}$ and $\Phi_{det}$ data were carried out for individual stations using two inversion schemes: (1) the layered-Earth model of Fischer and Le Quang (1981) and (2) the least-structure model of Constable *et al.* (1987). Parker's (1980) $D^+$ test indicated the absolute minimum $\chi^2$ misfit possible for the data from each site and aided the choosing of the suitable minimum misfit for either inverse scheme. The best-fitting models to the $\rho_{det}$ and $\Phi_{det}$ curves are illustrated for selected stations in Fig. 7, and given in pseudo-section form for all stations in Fig. 8. For the Fischer and Le Quang scheme, four layers were found to be sufficient to fit the data at stations 2, 4, 9, and 10, six layers at station 3, and five layers at the remaining stations. The resistivities and the depths of the layers varied even between neighbouring stations. Below a certain shallow depth the "plateaus" seen in the least-structure models are similar to the layered-Earth models in most cases. This indicates (as was noted by Jones *et al.* 1988) the presence of narrow layers with significantly different resisitivities both above and below them.

The $\rho_{det}$ and $\Phi_{det}$ variations at stations 1 and 2 are similar; those for station 1 are shown in Fig. 7. Both stations lie in the resistive region of the survey area, i.e., in the MacDonald Range (see Fig. 2). Station 3 lies near the boundary of the MacDonald Range and the Flathead Basin and required six layers to derive a layered-Earth model fitting the MT data. As seen in Fig. 7, there are several distinct layers, and the average resistivities of these are smaller than those under stations 1 and 2 by an order of magnitude or more. However, these 1D models for site 3 must be treated with caution, as the data from that site are obviously affected by the close proximity of the regional 2D structures.

The $\rho_{det}$ and $\Phi_{det}$ data of station 6 are typical of the Flathead Basin stations, where low-resistivity Cenozoic sediments extend to a depth of 2 km or more. At this depth the sediments below station 6 appear to be of particularly low resistivity. Below this, the resistivity gradually increases by an order of magnitude or more until depth about 5–6 km under stations 4–6 and depth ~20 km under stations 7 and 8. At greater depths is a zone of low resistivity in the middle to lower crust. Some 300 km to the north in the Rocky Mountain Trench (RMT), Hutton *et al.* (1987) also found a highly conductive (2–10 $\Omega \cdot$ m) layer, about 12 km thick, beneath the Trench sediments.

Stations 9–12 lie on the Lewis thrust sheet, east of Flathead Basin, and station 11 (Fig. 7) is representative of the $\rho_{det}$ and $\Phi_{det}$ data there. All four stations show distinctly the presence of a zone of very low resistivity at a depth of 3.5 ± 1 km. This layer corresponds to Mesozoic strata underlying Precambrian rocks of the Lewis thrust sheet and overlying Paleozoic rocks (see the cross section in Fig. 2). The Paleozoic basement in this area is somewhat less resistive than the surface rocks of the Lewis thrust sheet.

Figure 8 illustrates the 2D composite of the 1D layered-Earth

FIG. 6. Pseudosection of the reversed in-phase transfer function due to northwest–southeast-directed current flow. Red and blue indicate induction arrows pointing east and west respectively.

FIG. 8. Determinant resistivity $\rho_{det}$ pseudosection from all stations in the survey region. These are obtained from the data of best-fitting layered-Earth model curves (Fischer and Le Quang 1981) described in the text. Blue and red colours indicate, respectively, the resistive and conductive regions.

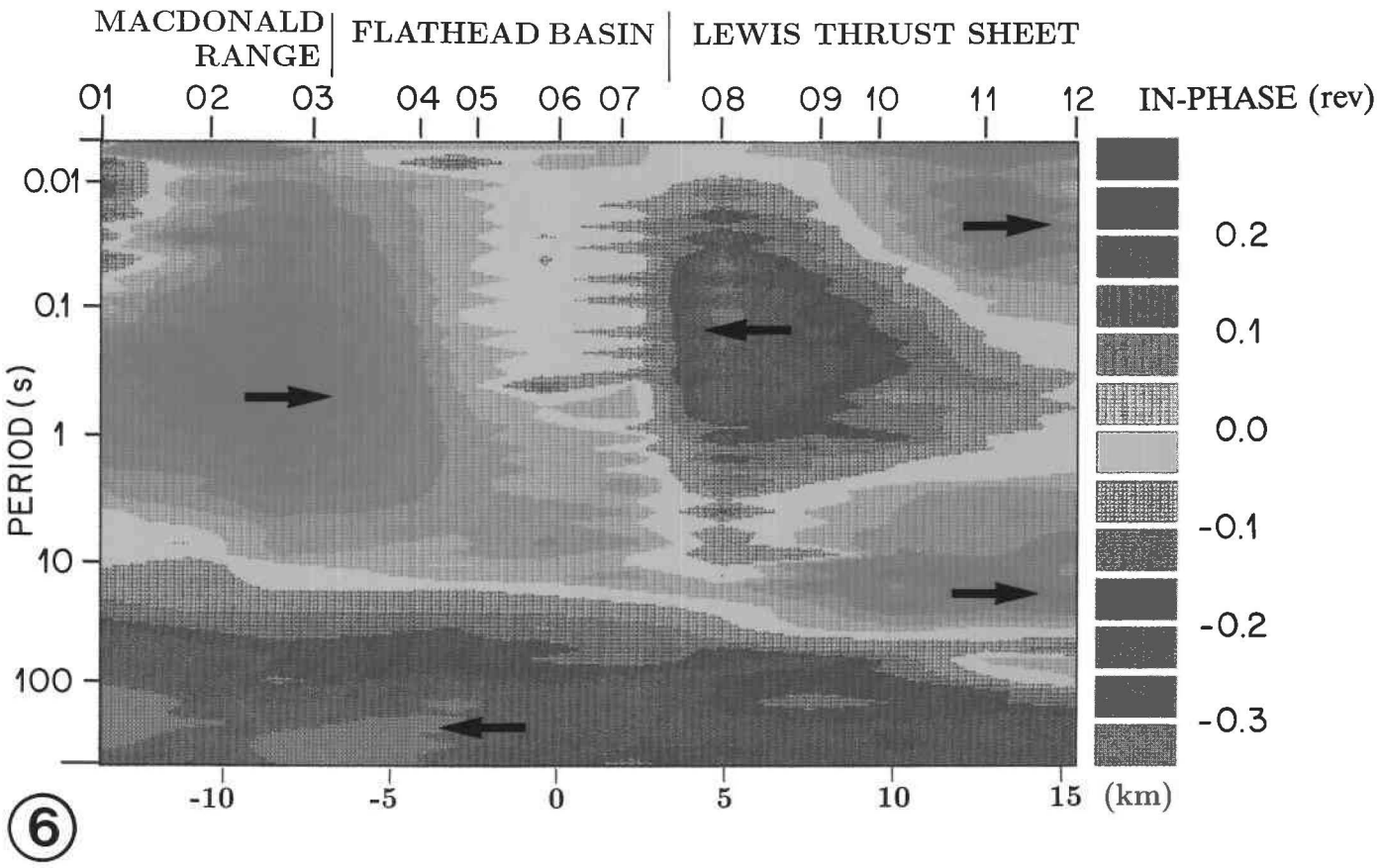
MACDONALD RANGE
FLATHEAD BASIN
LEWIS THRUST SHEET
01 02 03 04 05 06 07 08 09 10 11 12
IN-PHASE (rev)
0.2
0.1
0.0
-0.1
-0.2
-0.3
PERIOD (s)
0.01
0.1
1
10
100
-10 -5 0 5 10 15 (km)

6

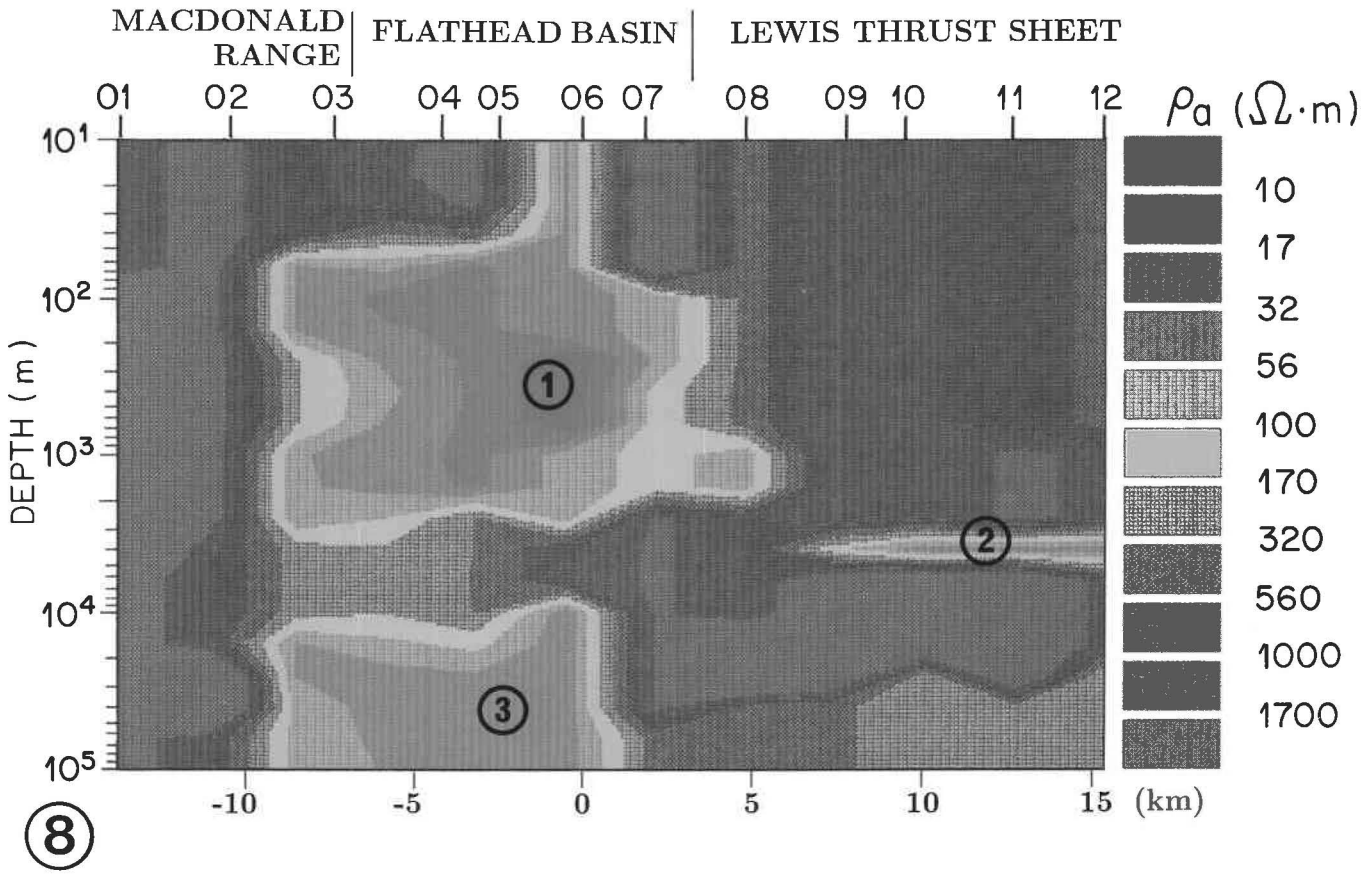
MACDONALD RANGE
FLATHEAD BASIN
LEWIS THRUST SHEET
01 02 03 04 05 06 07 08 09 10 11 12
ρa (Ω·m)
10
17
32
56
100
170
320
560
1000
1700
DEPTH (m)
10¹
10²
10³
10⁴
10⁵
1
2
3
-10 -5 0 5 10 15 (km)

8

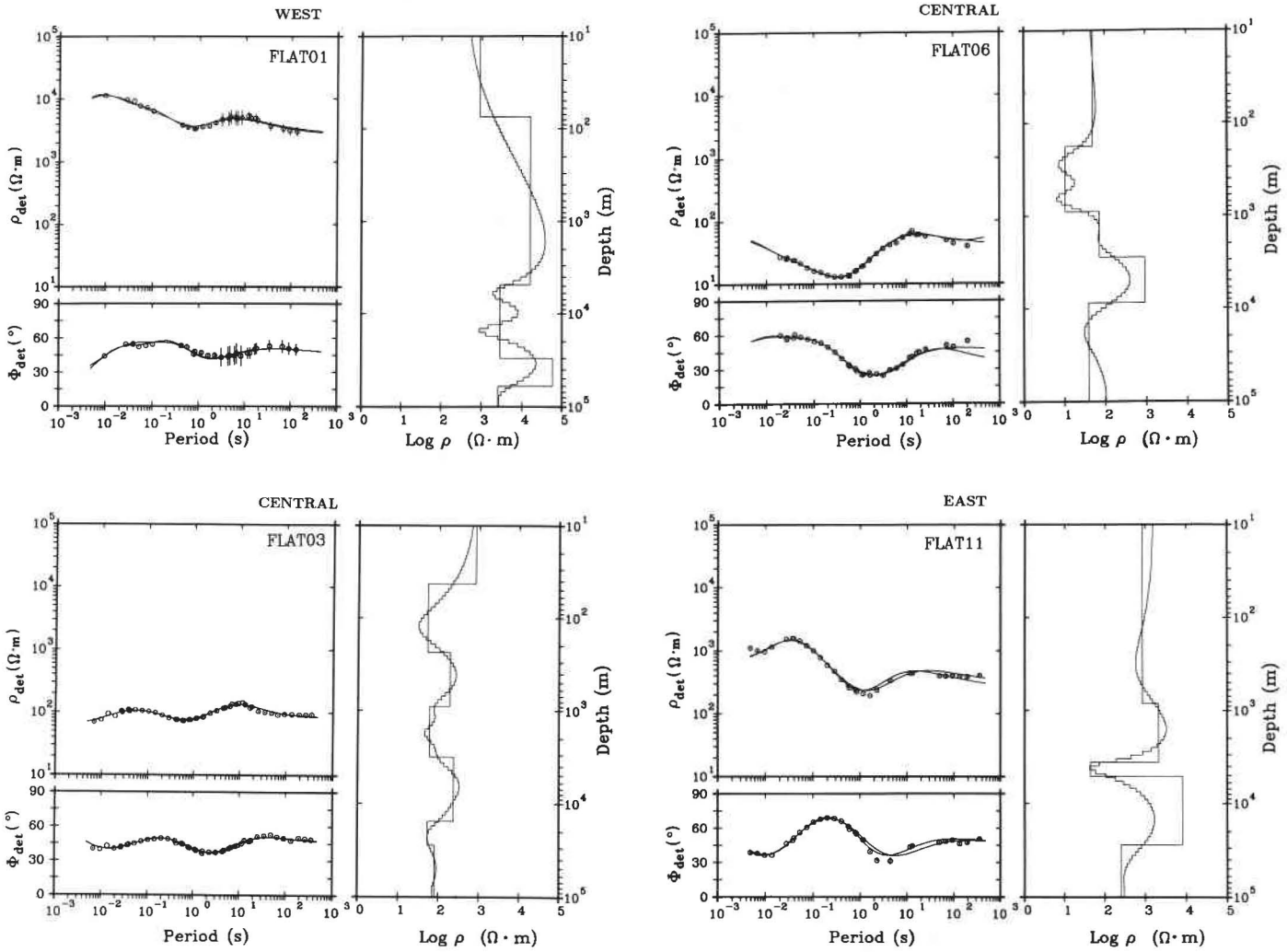


FIG. 7. $\rho_{det}$ and $\Phi_{det}$ values as a function of period at four selected stations along with the best-fitting layered-Earth models (steps) from the inversion scheme of Fischer and Le Quang (1981) and least-structure models (continuous small steps) from the algorithm of Constable *et al.* (1987). Note that the curves superimposed on the data points from both schemes are almost identical.

models from the determinant impedances (Fischer and Le Quang 1981) mentioned above. In this figure, blue represents the resistive regions and red the conductive ones. The figure clearly demonstrates the complexity of the Earth's structure in the survey area and suggests the presence of three major conducting features below the survey profile. These are (1) the Tertiary sediments of the Flathead Basin, (2) the Mesozoic clastics beneath the Lewis thrust sheet to the east, and (3) a middle to lower crustal conducting anomaly, beginning at approximately 10 km beneath the Flathead Basin. Although the quantitative results may be suspect, as we have undertaken an 1D inversion of 2D or 3D data and have not taken static shift effects into account, the qualitative results regarding the existence of these three gross structural resistivity anomalies are, in our opinion, not amendable to any other interpretation.

## Two-dimensional models

In their investigations of the resistivity structure of the Canadian Cordillera and the Alberta Basin using geomagnetic arrays, Ingham *et al.* (1987) noted that the gross geological structure of the region is 2D. The real induction arrows at several stations in this region pointed southwest, i.e., at right angles to the structural trend (Bingham *et al.* 1985). On the basis of this and other information, Ingham *et al.* (1987) considered this region to be a reasonable candidate for 2D modelling.

For our profile, the transfer function information of Fig. 6 and the $\rho_{det}$ pseudosection of Fig. 8 indicate the presence of three main conductive zones in the survey area (see above). The 1D modelling and the transfer function pseudosections aid in locating anomalies and defining their conductance but they do not determine the true depths of the conductive zones. To determine a valid quantitative model, we undertook a 2D numerical trial-and-error modelling study using Madden's EMCDC code (Madden 1973). We concentrated our attention on the transfer function and phase information from all 12 locations and on the apparent resistivity data from the sites within the Flathead Basin that were considered to be little affected by static shifts. Also, given that E-polarization data are more stable than B-polarization ones in the presence of small 3D structures, we preferentially fit these. The E- and B-polarization responses were calculated at 10 periods between 0.01 and 312.5 s and interpolated for contouring.

Modelling was initiated by using only the known geological

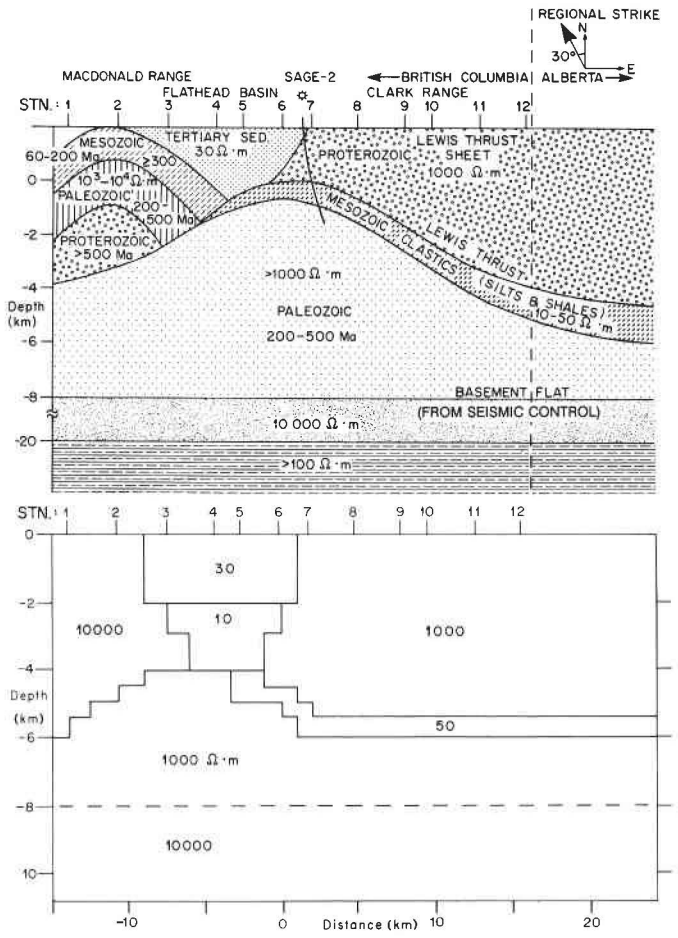


FIG. 9. (Upper part) Approximate geological features of the survey area that crosses the MacDonald Range, Flathead Basin, and Lewis thrust sheet, along with appropriate resistivities of the rock types. (Lower part) Model of the Earth structure based on the above geological features.

features of the area (Fig. 9, upper part) and the resistivities of various rock groups available from the literature (Fig. 9, lower part). However, this model produced MT responses that were very different from the observed ones. Thus, in constructing a more appropriate initial 2D model, we relied on the information provided by the 1D models and the pseudosections with respect to the geometry and the resistivities of the geoelectric structure. The goal was to obtain a model that produces MT and transfer function responses similar to those observed and yet incorporates the known geological characteristics of the area. Since the reasonably well determined field data are between 0.01 and 100 s, no attempt was made to model surficial or upper mantle features. Nearly 500 models were investigated to obtain one that produced E-polarization apparent resistivity and phase responses that matched reasonably well those that were observed. This final model, shown in Fig. 10, could not, however, produce B-polarization responses that clearly match the observations at all sites and at all periods.

The final model was derived by initially matching the short-period MT responses from the model with the observations at the Flathead Basin stations, assuming the resistivities of the host and the Flathead Basin to be 1500 and 35 $\Omega \cdot$ m respectively. Blocks of different resistivities were first added to match the responses at eastern stations and finally more blocks were

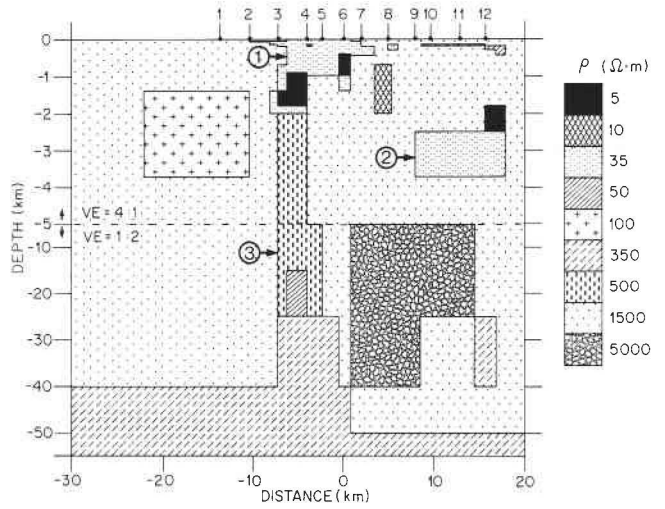


FIG. 10. Adopted model for the survey area with three major conductors, namely (1) Flathead Basin (35 $\Omega \cdot$ m), (2) Mesozoic strata (35 $\Omega \cdot$ m) on the eastern side of the survey area, and (3) lower crustal anomaly (500 $\Omega \cdot$ m) below the Flathead Basin.

added and adjusted to match E-polarization responses at longer periods. In the final model the lithosphere below 100 km is assumed to have a resistivity of 100 $\Omega \cdot$ m. The Flathead Basin and Mesozoic strata are modelled with a resistivity of 35 $\Omega \cdot$ m and the lower crustal anomaly beneath the basin, 500 $\Omega \cdot$ m, with an additional small conduction zone (50 $\Omega \cdot$ m) at a depth of 10 km. Following Bally *et al.* (1966), the depth of the Flathead Basin was taken to be about 2 km. Two conducting zones (5 $\Omega \cdot$ m) were placed near its base to make it as conducting as required by the field data at stations 4 and 6. At depths greater than 25 km, a moderately resistive layer (350 $\Omega \cdot$ m) overlaid a conducting half-space (100 $\Omega \cdot$ m). The Phillips and Gateway formations (see section on magnetotelluric data and analysis) are represented by narrow strata of 35 and 50 $\Omega \cdot$ m in the eastern part of the model. Below stations 1 and 2 at a depth of 2.5 ± 1 km, a conducting zone (100 $\Omega \cdot$ m) was placed to represent Cambrian sandstones and pebble conglomerates of the Flathead Formation that are found near that depth (Price 1962).

The resistivity and phase data calculated in the geological strike direction, and shown in Fig. 4, are reproduced for six representative stations of the survey area in Fig. 11 by circles (E polarization) and diamonds (B polarization). Superimposed on these are the model responses for E polarization (solid line) and B polarization (broken line). As mentioned earlier, the observed phase data are little influenced by near and far inhomogeneities, and are therefore more reliable than the apparent resistivity data. Figure 11 shows that the E-polarization phase responses of the model and of the data match extremely well at almost all of the stations in the period range 0.01–100 s. The resistivity responses also match very well, although at stations 1 and 9 (not shown) the observed data are static shifted upwards by a significant amount over the entire period range. Some of the differences between the observed and model apparent resistivity data may be due to static shift (e.g., at stations 3, 6, and 12), but at long periods the observed differences are due to the 3D influences that probably prevail in the survey area.

Blocks of reduced resistivity placed to the west to represent conductors imaged by Gough and his colleagues (e.g., the Canadian Cordilleran Regional (CCR) conductor, the southern Alberta – British Columbia (SABC) conductor, and the northern

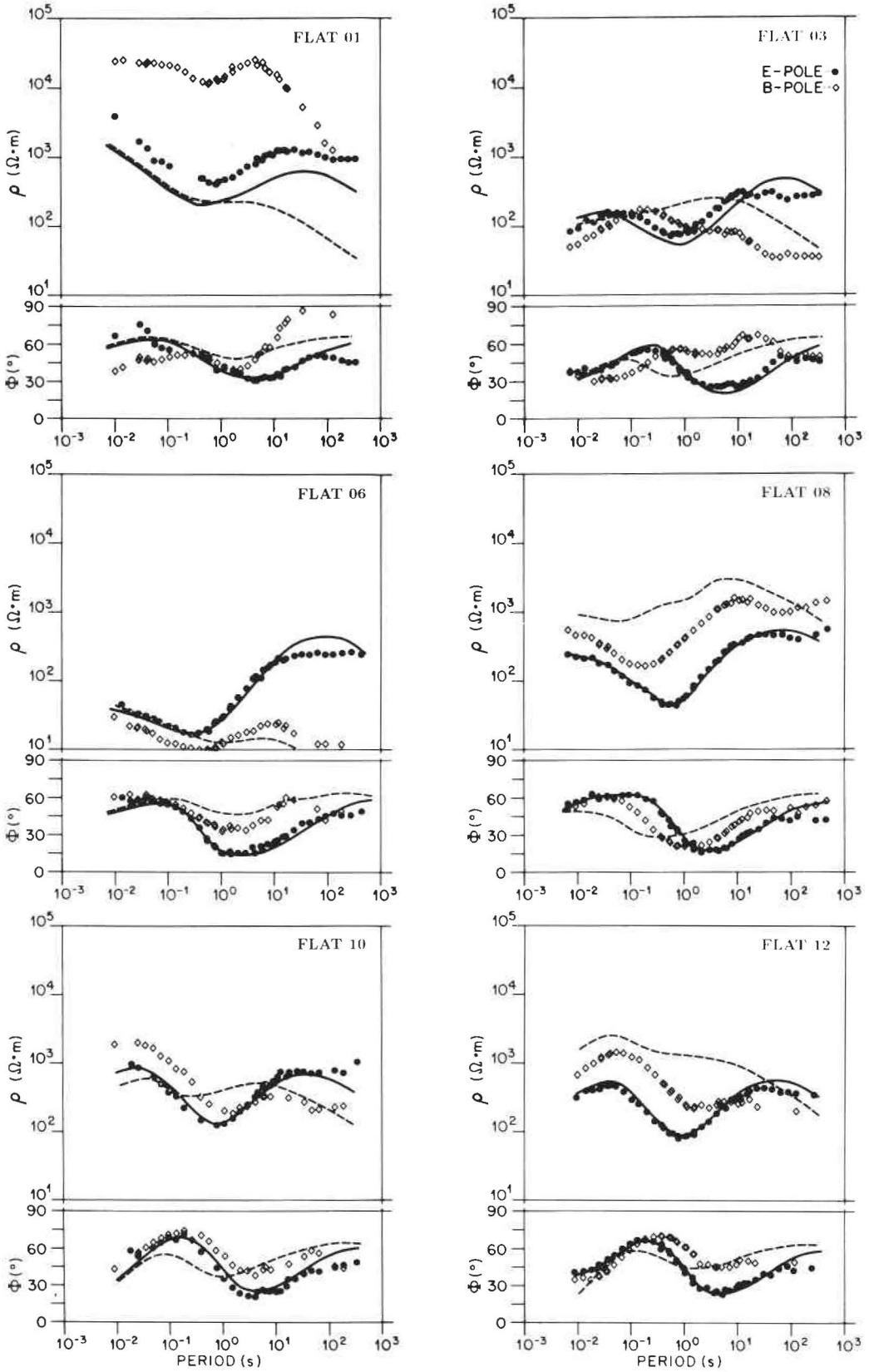


FIG. 11. Comparison of the calculated apparent resistivity and phase at N30°W (circles, E polarization) and N60°E (diamonds, B polarization) with the responses of the model (solid line, E polarization; broken line, B polarization) shown in Fig. 10 at six representative stations.

Rockies (NR) conductive ridge conductor (Gough *et al.* 1982; Ingham 1987)) proved to be too distant to have any significant influence on the calculated MT and transfer function responses.

To demonstrate further the capability of the model to represent the observations, a comparison is made between the phase pseudosection of the E-polarization response from the model and the phase pseudosection of the observed data (Fig. 12). Blue represents phases below 45°, signifying a transition from conductive to resistive structures with increasing depth, and red represents phases above 45°, signifying a transition from resistive to conductive structures with increasing depth. There is excellent agreement between the two pseudosections.

To understand the behaviour of the long-period transfer function responses (Fig. 6), we used a simplified version of the model shown in Fig. 10. In the new model (Fig. 13), the major conducting blocks were retained, with block no. 2 (Mesozoic strata) extended eastward to a distance of 50 km to account for the observed long-period transfer functions (an extended Mesozoic strata is supported by the red areas at the intermediate periods seen in the pseudosection of Fig. 6). This simplified model did not reproduce the MT responses as well as the model of Fig. 10. In the new model, a 7 $\Omega \cdot$m zone was placed 25–43 km from station 6 on the western side of the Flathead Basin at a depth of 1.5–3.7 km. Due to its location, this zone of anomalously low resistivity will henceforth be referred to as the MacDonald Range conductor (MRC). On its western side between 43 and 54 km, a body of equal resistivity was added to represent the RMT, which extends to the base of the crust as do some Cordilleran conductors mentioned above. The model of Fig. 13 produced long-period transfer functions that were quite close to components of the observations perpendicular to the structural trends in the area. This is shown in Fig. 14 where in-phase and quadrature components of the transfer functions for periods of 31.25, 100, and 312.5 s are compared with the observations for models of Fig. 10 (continuous line) and Fig. 13 (broken line). A shorter RMT conductor with its base at depths of 20–25 km does not fit the observations as well as one with its base at the crust–mantle boundary (35 km).

## Discussion and conclusion

A study of magnetotelluric and geomagnetic transfer function data from 12 sites located in the region of Flathead Basin has been carried out. Pseudosections and 1D models aided construction of an initial 2D model of the survey area, which required several smaller conductors to produce E-polarization apparent resistivity and phase variations that matched the observed data. Three major conducting bodies have been found and modelled:

1. The Flathead basin extending 10–12 km east-west between stations 3 and 7 and consisting of unconsolidated sediments (resistivity $\approx$ 35 $\Omega \cdot$m or less) to a depth of about 2 km in a very resistive ($\sim$ 1500 $\Omega \cdot$m) environment. The basin is more conducting beneath station 6 than elsewhere.
2. Mesozoic strata, which are comparable in resistivity to the sediments of the basin, lie at a depth of 3.5 $\pm$ 1 km on the eastern side of the Flathead Basin below the Lewis thrust sheet. They have been traced beneath stations 9–12 and may also exist to the east.
3. Below the Flathead Basin, and about equally as wide, is a lower crustal anomaly (LCA) that is less conductive than the sediments of the basin but extends deep into the lower crust and possibly beyond. A zone of enhanced conductivity in the middle to lower crust was also recently imaged beneath another sedimentary basin, namely the Williston Basin (Jones and Craven 1990). There may be some link between the locations of sedimentary basins and zones of weakness in the middle crust as imaged by enhanced electrical conductivity, e.g., structural control on the formation of basins.

The transfer function analysis showed that for short periods the direction of the induction arrows are effectively controlled by the conductive structures of the Flathead and Kishenehn basins. The transfer functions are noted to be significantly influenced by the conducting sediments of the Alberta Basin to the east. The directions of the long-period transfer functions did not, however, seem to be influenced by the Cordilleran conductors (CCR, SABC, and NR). Instead, the crustal conductors (RMT and MRC), at depths of $\sim$1.5 km and extending to 54 km on the western side of the Flathead Basin, produce at longer periods transfer functions that are quite close to the observed data.

Lower crustal conductors have also been reported at other localities, e.g., beneath the Andes (Schmucker *et al.* 1964), the Rockies (Porath and Gough 1971), the Canadian Appalachians (Bailey *et al.* 1974), and the Adirondacks (Connerney *et al.* 1980). The presence of hydrated rocks (Hyndman and Hyndman 1968) in the lower crust has been considered to be a possible cause of low resistivity there. However, work by Olhoeft (1981) showed that "hydrated" minerals are not intrinsically conducting; it is the fluids released by dehydration reactions that cause the reduced electrical resistivity. More recently, mantle upflow has been proposed by Gough (1984, 1986) to explain the low resistivity of the Cordilleran conductors. This may also be the cause of the low resistivity of LCA, RMT and MRC. According to Gough, high temperatures and partial melting exist in the uppermost mantle beneath most of the Intermontane and Ominica belts of the Canadian Cordillera between 49 and 54°N, and also under parts of the western United States, and there is an upcurrent of mantle circulation in these regions. The fluids, mantle-derived water and silicate melts produced by partial melting, rise locally into the middle and upper crust (with the water rising more than the silicate melts) and are trapped beneath an impermeable layer (Jones 1987; Kurtz *et al.* 1990). The presence of highly saline hot water in the interconnected pore spaces of the rocks causes the ionic conduction that Gough considers to be responsible for the low resistivity of the CCR. If partial melt fluids are present beneath the Flathead survey area, then our recognition of the LCA, RMT, and MRC conductors lends strong support to the mantle upflow hypothesis of Gough.

Some questions naturally arise. Is this mantle upflow also responsible for creation of the Flathead and the Kishenehn basins? Did the rising fluids cause a weakening of the lower crust, resulting in subsidence along the Flathead Fault and its antithetic Nyack Fault and creating the Flathead–Kishenehn Basin? Considerably more work must be done to answer these important questions.

FIG. 12. Phase pseudosections from the data calculated in the geological trend direction (upper) and from the 2D model (lower). Blue indicates phases below 45°—a transition from resistive to conductive structures with increasing depth.

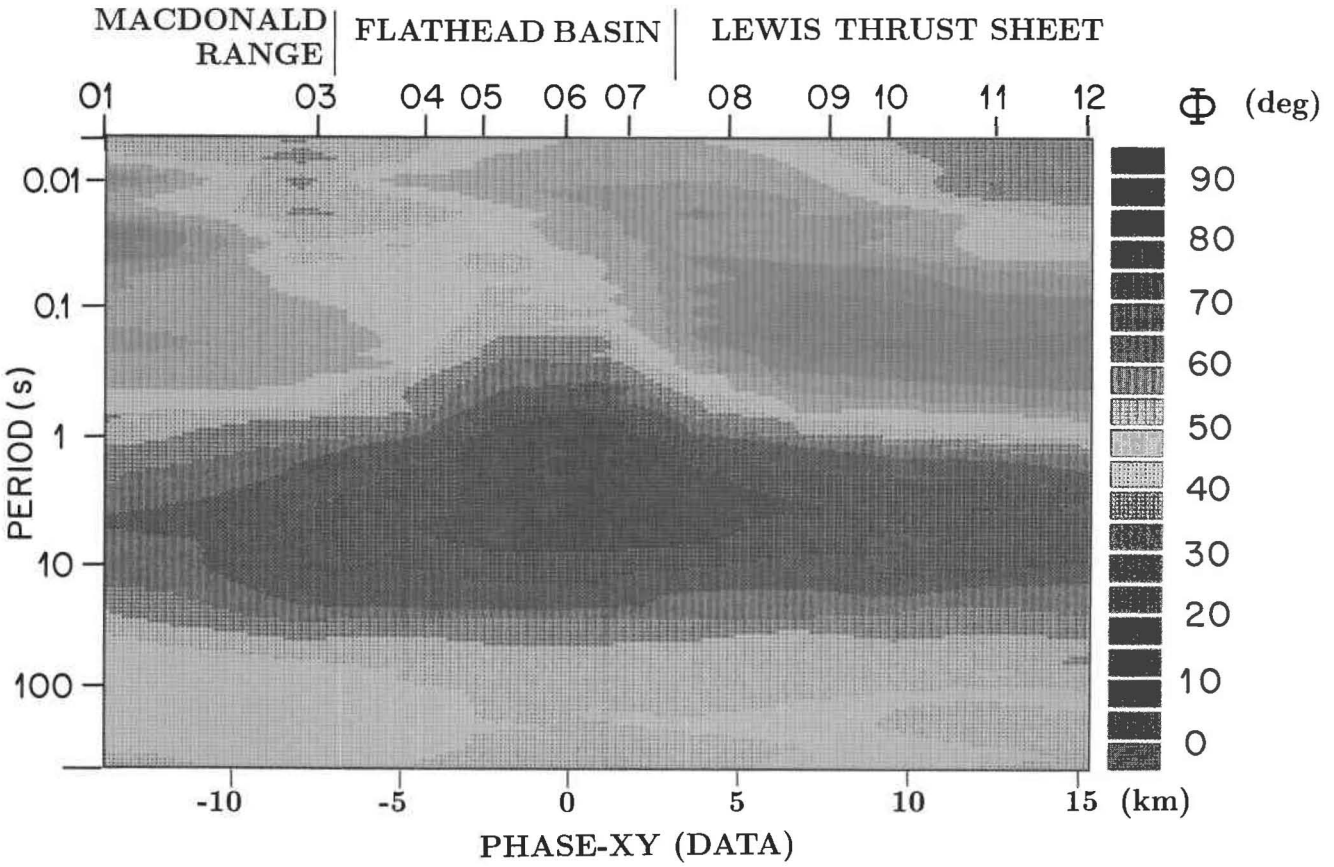
MACDONALD RANGE
FLATHEAD BASIN
LEWIS THRUST SHEET
01
03
04
05
06
07
08
09
10
11
12
Φ (deg)
0.01
0.1
1
10
100
PERIOD (s)
90
80
70
60
50
40
30
20
10
0
-10
-5
0
5
10
15
(km)
PHASE-XY (DATA)

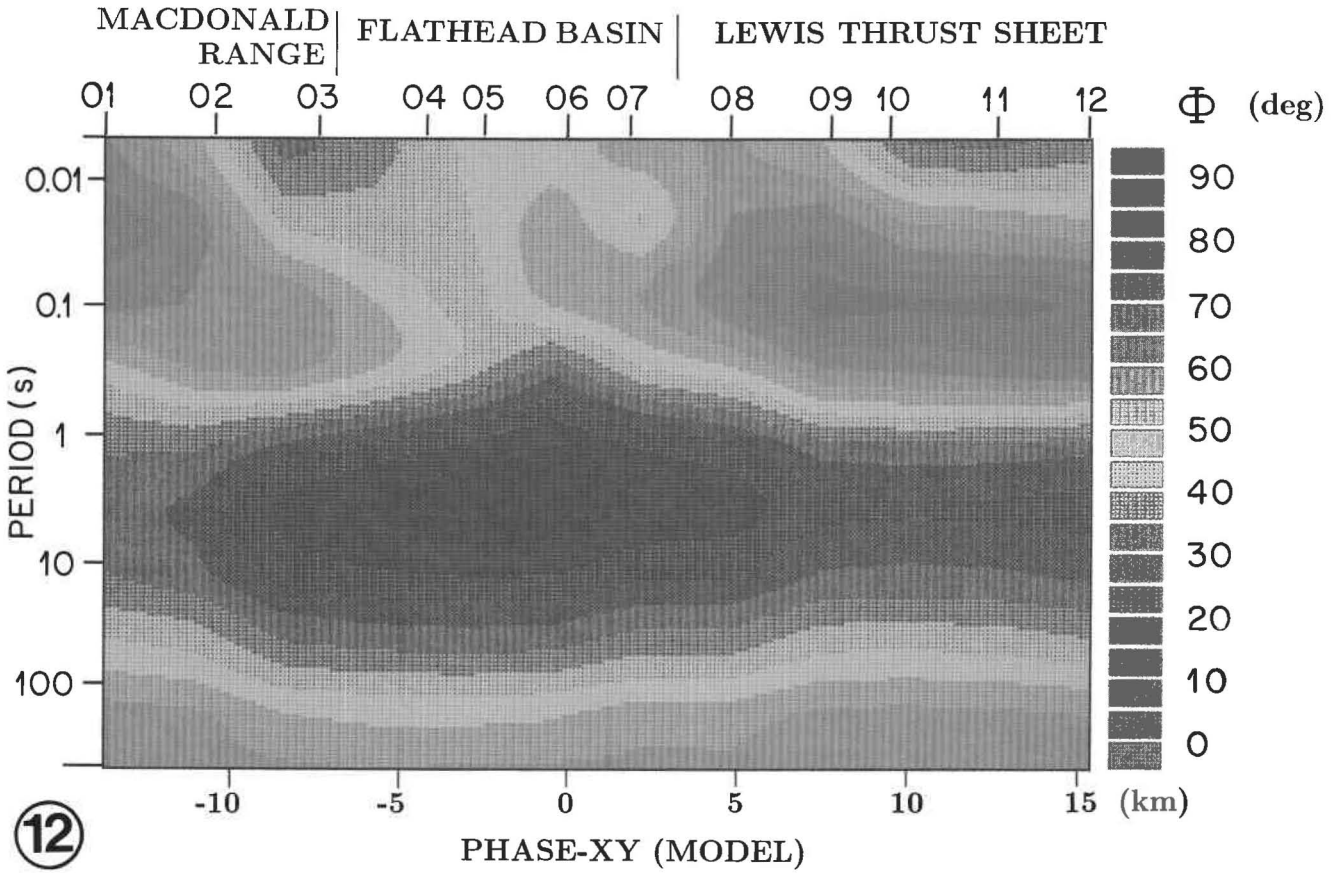
MACDONALD RANGE
FLATHEAD BASIN
LEWIS THRUST SHEET
01
02
03
04
05
06
07
08
09
10
11
12
Φ (deg)
0.01
0.1
1
10
100
PERIOD (s)
90
80
70
60
50
40
30
20
10
0
-10
-5
0
5
10
15
(km)
PHASE-XY (MODEL)

12

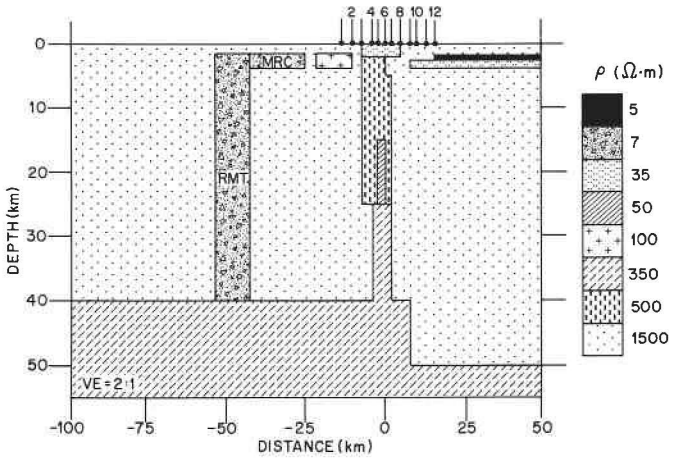


FIG. 13. Simplified model of the survey area with three major conductors of Fig. 10 (Mesozoic strata extended eastward to account for long-period transfer functions) and the additional new 7 Ω · m Macdonald Range conductor (MRC) and Rocky Mountain Trench conductor (RMT).

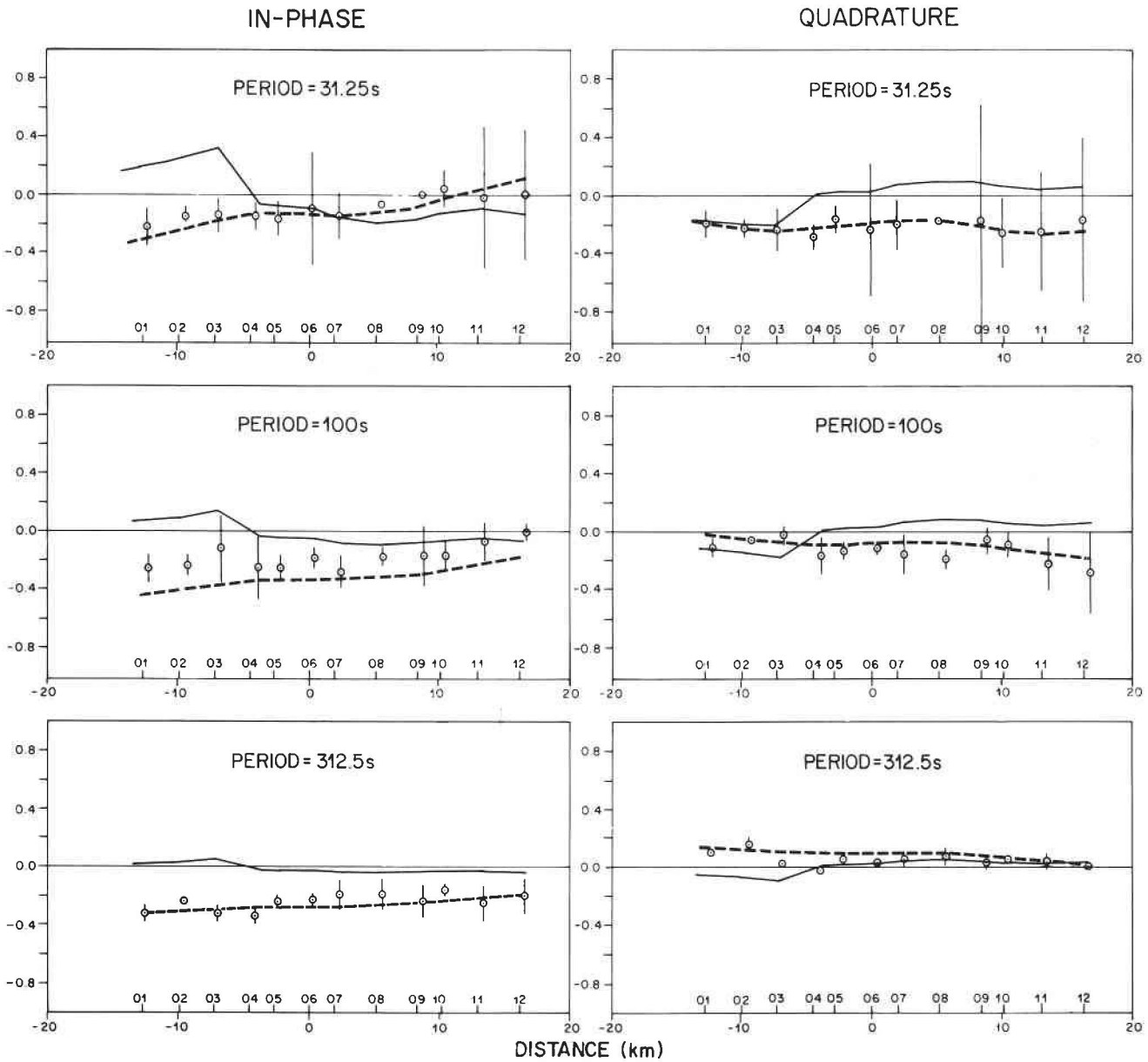


FIG. 14. Geomagnetic transfer functions computed for the models of Fig. 10 (solid line) and Fig. 13 (broken line). The projected transfer functions are at each site on a profile striking N60°E. The periods chosen are 31.25, 100, and 312.5 s.

## Acknowledgments

The data analyzed herein from the Flathead Basin were donated by Shell (Canada) Ltd. to Lithoprobe, and we wish to thank Mr. R. A. Charters of Shell for assistance regarding the data format and the regional structure as depicted in Fig. 9. We also acknowledge Drs. R. D. Kurtz and D. E. Boerner for valuable discussion during the course of this work. Drs. Gaston Fischer and Steve Constable provided their codes for the two one-dimensional inversions used, and we thank them both. This paper was improved by the editorial efforts of Dr. J. J. Clague, for which the authors are grateful.

BAILEY, R. C., EDWARDS, R. N., GARLAND, G. D., KURTZ, R., and PITCHER, D.H 1974. Electrical conductivity studies over a tectonically active area in eastern Canada. Journal of Geomagnetism and Geoelectricity, **26**: 125–146.

BALLY, A. W., GORDY, P. L., and STEWART, G. A. 1966. Structure, seismic data and orogenic evolution of southern Canadian Rocky Mountains. Bulletin of Canadian Petroleum Geology, **14**: 337–381.

BERDICHEVSKY, M. M., and DMITRIEV, V. I. 1976. Distortion of magnetic and electric fields by near-surface lateral inhomogeneities. Acta Geodaetica, Geophysica et Montanistica Hungarica, A Quarterly Journal of the Hungarian Academy of Sciences, **11**: 447–483.

BINGHAM, D. K., GOUGH, D. I., and INGHAM, M. R. 1985. Conductive structures under the Canadian Rocky Mountains. Canadian Journal of Earth Sciences, **22**: 384–398.

CHILDERS, M. O. 1964. Structure around Glacier National Park, Montana. Bulletin of Canadian Petroleum Geology, **12**: 378–382.

CONNERNEY, J. E. P., NEKUT, A., and KUCKES, A. F. 1980. Deep crustal electrical conductivity in the Adirondacks. Journal of Geophysical Research, **85**: 2603–2614.

CONSTABLE, S. C., PARKER, R. L., and CONSTABLE, C.G. 1987. Occam's inversion: a practical algorithm for generating models from electromagnetic sounding data. Geophysics, **52**: 289–300.

CONSTENIUS, K. 1982. Relationship between the Kishenehn Basin and the Flathead Listric Normal Fault system and Lewis Thrust Salient. *In* Geologic studies of the Cordilleran Thrust Belt. *Edited by* R. B. Powers. Rocky Mountain Association of Geologists, Denver, CO, pp. 817–830.

——— 1988. Structural configuration of the Kishenehn Basin delineated by geophysical methods, northwestern Montana and southeastern British Columbia. Mountain Geologist, **25**: 13–28.

EGGERS, D. E. 1982. An eigenstate formulation of the magnetotelluric impedance tensor. Geophysics, **47**: 1204–1214.

FISCHER, G., and LE QUANG, B. V. 1981. Topography and minimization of the standard deviation in one-dimensional magnetotelluric modelling. Geophysical Journal of the Royal Astronomical Society, **67**: 279–292.

GOUGH, D. I. 1984. Mantle upflow under North America and plate dynamics. Nature (London), **311**: 428–433.

——— 1986. Mantle upflow tectonics and the Canadian Cordillera. Journal of Geophysical Research, **91**: 1909–1919.

GOUGH, D. I., and INGHAM, M. R. 1983. Interpretation methods for magnetometer arrays. Reviews of Geophysics and Space Physics, **21**: 805–827.

GOUGH, D. I., BINGHAM, D.K., and INGHAM, M. R. 1982. Conductive structures in southwestern Canada: a regional magnetometer array study. Canadian Journal of Earth Sciences, **19**: 1680–1690.

GUPTA, J. C., KURTZ, R.D., and CAMFIELD, P. A. 1983. An induction anomaly near the west coast of Hudson Bay, Canada. Geological Survey of Canada, Earth Physics Branch, Open File 83–29.

GUPTA, J. C., KURTZ, R.D., CAMFIELD, P. A., and NIBLETT, E. R. 1985. A geomagnetic induction anomaly from IMS data near Hudson Bay, and its relation to crustal electrical conductivity in central North America. Geophysical Journal of the Royal Astronomical Society, **81**: 33–46.

HUTTON, V. R. S., DAWES, G. J. K., DEVLIN, T., and ROBERTS, R. 1985. A broadband tensorial magnetotelluric study in the Travale–Radicondoli geothermal field. Geothermics, **14**: 645–652.

HUTTON, V. R. S., GOUGH, D. I., DAWES, G. J. K., and TRAVASSOS, J. 1987. Magnetotelluric soundings in the Canadian Rocky Mountains. Geophysical Journal of the Royal Astronomical Society, **90**: 245–263.

HYNDMAN, R. D., and HYNDMAN, D. W. 1968. Water saturation and high electrical conductivity in the lower crust. Earth and Planetary Science Letters, **4**: 427–432.

INGHAM, M. R. 1987. Models of conductive structure under the Canadian Cordillera. Geophysical Journal of the Royal Astronomical Society, **88**: 477–485.

——— 1988. The use of invariant impedances in magnetotelluric interpretation. Geophysical Journal of the Royal Astronomical Society, **92**: 165–169.

INGHAM, M. R., GOUGH, D. I., and PARKINSON, W. D. 1987. Models of conductive structure under the Canadian Cordillera. Geophysical Journal of the Royal Astronomical Society, **88**: 477–485.

JONES, A. G. 1981. Geomagnetic induction studies in Scandinavia—II. Geomagnetic depth sounding, induction vectors and coast effect. Journal of Geophysics, **50**: 23–36.

——— 1986. Parkinsons' pointers' potential perfidy! Geophysical Journal of the Royal Astronomical Society, **87**: 1215–1224.

——— 1987. MT and refection: an essential combination. Geophysical Journal of the Royal Astronomical Society, **89**: 7–18.

——— 1988. Static shift of magnetotelluric data and its removal in a sedimentary basin environment. Geophysics. **53**: 967–978.

JONES, A. G., and CRAVEN, J. A. 1990. The North American Central plains conductivity anomaly and its correlation with gravity, magnetics, seismic, and heat flow data in the Province of Saskatchewan. Physics of the Earth and Planetary Interiors, **60**: 169–194.

JONES, A. G., KURTZ, R. D., OLDENBURG, D. W., BOERNER, D. E., and EILLIS, R. 1988. Magnetotelluric observations along the LITHOPROBE southeastern Canadian Cordilleran transect. Geophysical Research Letters, **15**: 677–680.

KURTZ, R. D., DELAURIER, J M., and GUPTA, J. C. 1990. The electrical conductivity distribution beneath Vancouver Island: a region of active plate subduction. Journal of Geophysical Research. (In press.)

MADDEN, T. R. 1973. Instruction manual for EMCDC and EMUVC (EMCAL). Exploration Aids Inc., Needham, MA.

MUDGE, M. R. and EARHART, R.L. 1980. The Lewis Thrust Fault and related structures in the disturbed belt, northwestern Montana. United States Geological Survey, Professional Paper 1174.

OLHOEFT, G. R. 1981. Electrical properties of granite with implications for the lower crust. Journal of Geophysical Research, **86**: 931–936.

PARK, S.K., and LIVELYBROOKS, D. 1989. Quantitative interpretation of rotationally invariant parameters in magnetotellurics. Geophysics, **54**: 1483–1490.

PARKER, R. . 1980. The inverse problem of electromagnetic induction: existence and construction of solutions based on incomplete data. Journal of Geophysical Research, **85**: 4421–4425.

PORATH, H., and GOUGH, D. I. 1971. Mantle conductive structures in the western United States from magnetometer array studies. Geophysical Journal of the Royal Astronomical Society, **22**: 261–275.

PRICE, R. A. 1962. Fernie map-area, east half, Alberta and British Columbia; 82G east half. Geological Survey of Canada, Paper 61–24 (includes Map 35–1961).

——— 1981. The Cordilleran foreland thrust and fold belt in the southern Canadian Rocky Mountains. *In* Thrust and nappe tectonics. *Edited by* K. R. McClay and N. J. Price. Geological Society of London, Special Publication 9, pp. 427–448.

RANGANAYAKI, R. P. 1984. An interpretive analysis of magnetotelluric data. Geophysics, **49**: 1730–1748.

REDDY, I. K., and RANKIN, D. 1972. On the interpretation of magnetotelluric data in the plains of Alberta. Canadian Journal of Earth Sciences, **9**: 514–527.

SCHMUCKER, U. 1970. Anomalies of geomagnetic variations in the southwestern United States. Bulletin of the Scripps Institution of Oceanography, no. 13.

SCHMUCKER, U., HARTMANN, O., GIESECKE, A. A., JR., CASAVERDE, M., and FORBUSH, S. E. 1964. Electrical conductivity anomaly in the Earth's crust in Peru. Carnegie Institution of Washington, Yearbook **63**: pp. 354–362.

STERNBERG, B. K., WASHBURNE, J.C., and PELLERIN, L. 1988. Correction for the static shift in magnetotellurics using transient electromagnetic soundings. Geophysics, **53**: 1459–1468.

SULE, P. O., and HUTTON, V.R. S. 1986. A broad-band magnetotelluric study in southeastern Scotland. Data acquisition, analysis and one-dimensional modelling. Annales Geophysicae, Series B, **4**: 145–156.